

# Mechanical and Flame-Retarding Properties of Styrene-Butadiene Rubber Filled with Nano-CaCO<sub>3</sub> as a Filler and Linseed Oil as an Extender

S. Mishra, N. G. Shimpi

Department of Chemical Technology, North Maharashtra University, Jalgaon, P.O. Box 80, M.S. India 425 001

Received 26 October 2004; accepted 14 March 2005

DOI 10.1002/app.22458

Published online in Wiley InterScience (www.interscience.wiley.com).

**ABSTRACT:** A nanosize CaCO<sub>3</sub> filler was synthesized by an *in situ* deposition technique, and its size was confirmed by X-ray diffraction. CaCO<sub>3</sub> was prepared in three different sizes (21, 15, and 9 nm). Styrene-butadiene rubber (SBR) was filled with 2–10 wt % nano-CaCO<sub>3</sub> with 2% linseed oil as an extender. Nano-CaCO<sub>3</sub>-SBR rubber composites were compounded on a two-roll mill and molded on a compression-molding machine. Properties such as the specific gravity, swelling index, hardness, tensile strength, abrasion resistance, modulus at 300% elongation, flame retardancy, and elongation at break were measured. Because of the reduction in the nanosize of CaCO<sub>3</sub>, drastic improvements in the mechanical properties were found. The size of 9 nm showed the highest increase in the tensile strength (3.89 MPa) in comparison with commercial CaCO<sub>3</sub> and the two other sizes of

nano-CaCO<sub>3</sub> up to an 8 wt % loading in SBR. The elongation at break also increased up to 824% for the 9-nm size in comparison with commercial CaCO<sub>3</sub> and the two other sizes of nano-CaCO<sub>3</sub>. Also, these results were compared with nano-CaCO<sub>3</sub>-filled SBR without linseed oil as an extender. The modulus at 300% elongation, hardness, specific gravity, and flame-retarding properties increased with a reduction in the nanosize with linseed oil as an extender, which helped with the uniform dispersion of nano-CaCO<sub>3</sub> in the rubber matrix. © 2005 Wiley Periodicals, Inc. *J Appl Polym Sci* 98: 2563–2571, 2005

**Key words:** nanocomposites; styrene butadiene rubber; nano-CaCO<sub>3</sub>

## INTRODUCTION

Carbon black used to be the most important reinforcing agent in the rubber material industries. However, it is polluting in nature, so most researchers have tried to investigate satisfactory reinforcing agents. It is well known that the particle size, structure, and surface characteristics are important parameters that determine the reinforcing ability of a filler; the particle size is especially important because a reduction in size provides a greater surface area.<sup>1</sup> The reinforcing ability of clay is poor because of its big particle size and low surface activity. It is of great interest to use inorganic fillers (talc, nano-ZnO, nano-CaCO<sub>3</sub>, nano-CaSO<sub>4</sub>, and nano-Al<sub>2</sub>O<sub>3</sub>) as substitutes for carbon black in rubber compounding.<sup>2</sup> Recently, according to developments in nanotechnology, there has been a growing interest in the field of nanocomposites because of their special property enhancement.<sup>3–7</sup> Nanocomposites possess unique properties that are not shared by conventional composites, primarily because

of their large interfacial area per unit of volume.<sup>8</sup> Nanocomposites show superior physical and mechanical behavior over conventional microcomposites and, therefore, offer new techniques and business opportunities.<sup>9</sup>

Oils are used as extenders in rubber composites and generally serve two purposes: (1) the homogeneous mixing of nanoparticles is possible with the addition of oils and (2) crack propagation due to filler addition can be reduced and so an improvement in the properties is observed. Linseed oil is the best extender used by the rubber industries because the linolic concentration is higher. Hence, attachment with other organic groups is possible. The purpose of this study was to investigate the effect of linseed oil and nanoparticles of CaCO<sub>3</sub> on the mechanical properties of styrene-butadiene rubber (SBR).

## EXPERIMENTAL

### Materials

SBR (Raj polymer, Ghatkoper, Mumbai, India) was used. The physical properties of SBR are listed in Table I. The rubber additives, namely, stearic acid, zinc oxide (ZnO), zinc diethyl dithiocarbamate (ZDC), 2,2'-dibenzothiazyl disulfide (MBTS), vulconex, and

Correspondence to: S. Mishra (profsm@rediffmail.com).

Contract grant sponsor: Indian Space Research Organization/University of Pune.

TABLE I  
Physical Properties of SBR

No.	Property	Value
1	Appearance	Light tan/bale
2	Bound styrene	23.5%
3	Organic acid	6.5%
4	Mooney viscosity	50 mL (100°C)
5	Specific gravity	0.94 g/cc

sulfur, were commercial-grade and were procured from Bayer India, Ltd. (Mumbai, India; Table II). Analytical grades of calcium chloride, potassium bicarbonate, and poly(ethylene glycol) (PEG; molecular weight = 6000) were procured from Qualigens India, Ltd. (Mumbai, India), and were used for the synthesis of nanoparticles of calcium carbonate. The linseed oil was cold-pressed oil with the following concentrations of fatty acids: 6.2% palmitic, 15.1% linoleic, 5.8% stearic, 49.9% linolenic, and 22% oleic. The specific gravity of the linseed oil was 0.927. The particle size of the commercial  $\text{CaCO}_3$  was 20  $\mu\text{m}$ .

### Nanoparticle synthesis

Nanosize calcium carbonate was synthesized by an *in situ* deposition technique. Calcium chloride (110 g by weight) was placed in 100 mL of water; 248 g (by weight) of PEG was diluted in 100 mL of water and was mildly heated for proper mixing. A complex of calcium chloride and PEG was prepared in molar ratios of 1 : 4, 1 : 20, and 1 : 32. Another solution of  $\text{K}_2\text{CO}_3$  was prepared, with 106 g placed in 100 mL of distilled water. The first complex was digested for 12 h, and then the solution of  $\text{K}_2\text{CO}_3$  was added slowly; the mixture was again kept for digestion for 12 h. The precipitate was filtered, washed with water, and dried in a vacuum drier.<sup>10–16</sup> Nanosynthesis by the *in situ* deposition technique is shown in Figure 1. The X-ray diffraction (XRD) grams of nanoparticles of  $\text{CaCO}_3$  were recorded on a Miniflex instrument (Rigaku, Tokyo, Japan). The value of  $2\theta$ , that is, the diffraction peak, was 28.600.

TABLE II  
Formulation of SBR Used in the Composite Preparation

SBR	100 g
Stearic acid	3 g
ZnO	3 g
Vulconex	1 g
ZDC	0.5 g
MBTS	0.5 g
Sulfur	1.8 g
Linseed oil	2 g
Nano- $\text{CaCO}_3$	Variable

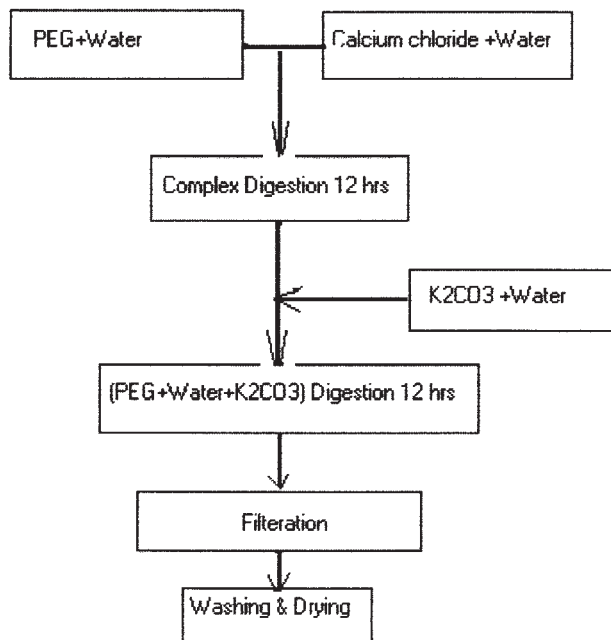


Figure 1 *In situ* deposition method for nano- $\text{CaCO}_3$  synthesis.

### Preparation of the rubber nanocomposites

Rubber was masticated for 2–3 min, and then stearic acid was added to give flexibility to the raw rubber. After the complete addition of stearic acid, ZnO was added during the mastication process. After the addition of ZnO, MBTS and ZDC, acting as accelerators, were added to the rubber, which was masticated for 1–2 min. Later, vulconex was added as an antioxidant. After sufficient mastication, sulfur was added. At last, the nano- $\text{CaCO}_3$  filler with and without linseed oil was added very carefully. The compounded rubber was subjected to compression molding for 40 min at 140°C under 100 kg/cm<sup>2</sup> of pressure to produce a square sheet (15 cm × 15 cm × 0.3 cm).

### Mechanical testing

The cured sheets were subjected to conditioning for 24 h at a relative humidity of 50%. The mechanical properties, such as the tensile strength, elongation at break, and modulus at 300%, were measured per ASTM D 412 with a universal testing machine (UTM 2302) supplied by R&D Equipment (Mumbai, India). The crosshead speed was 50 mm/min. The samples were the standard dumbbell shape. All measurements were performed eight times to obtain an average value.

### Hardness testing

The compression-molded specimens were tested to report hardness data with a Shore A hardness tester per ASTM D 2240.

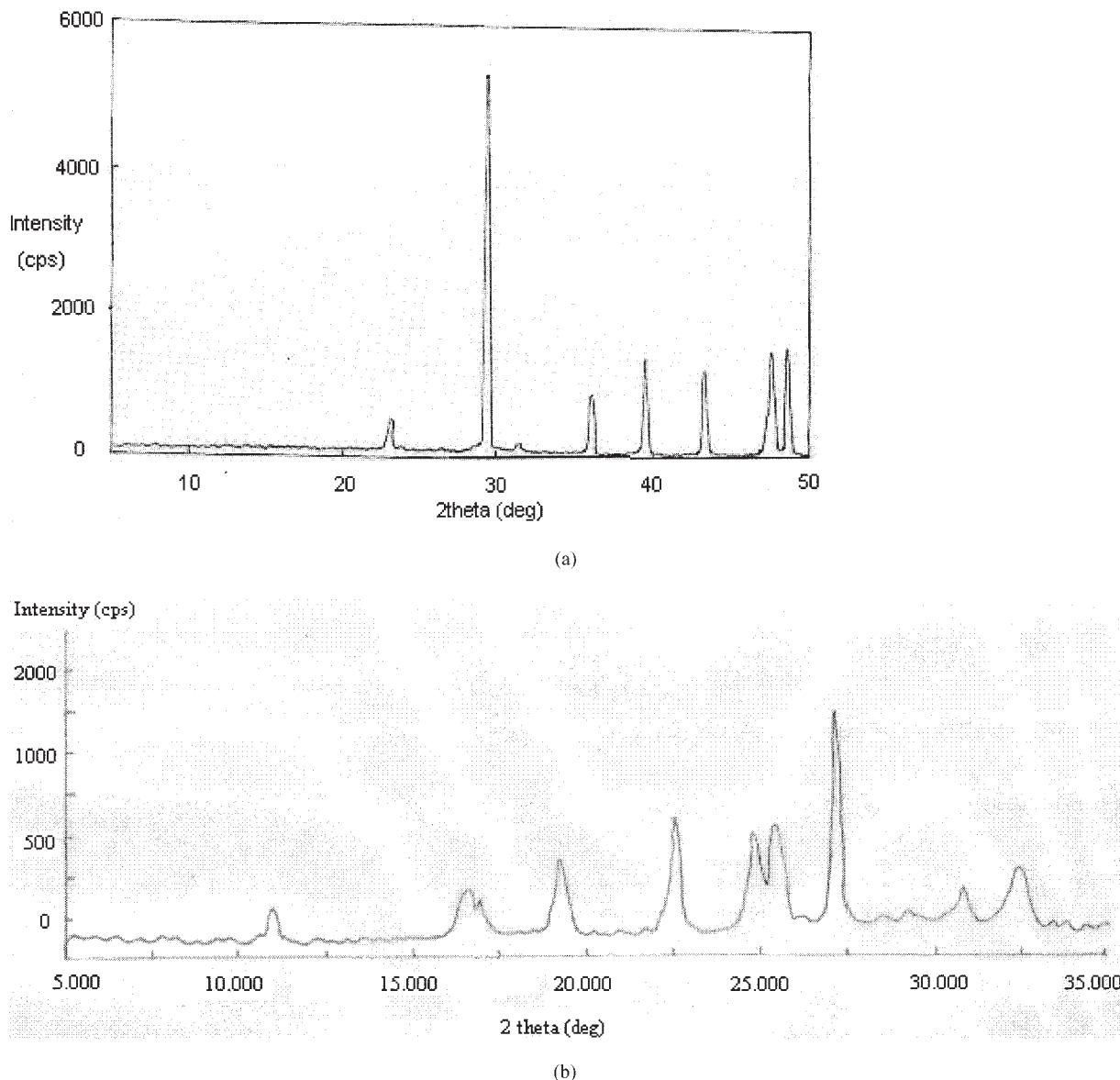


Figure 2 XRD grams of (a) 21-, (b) 15-, and (c) 9-nm CaCO<sub>3</sub>.

**Specific gravity**

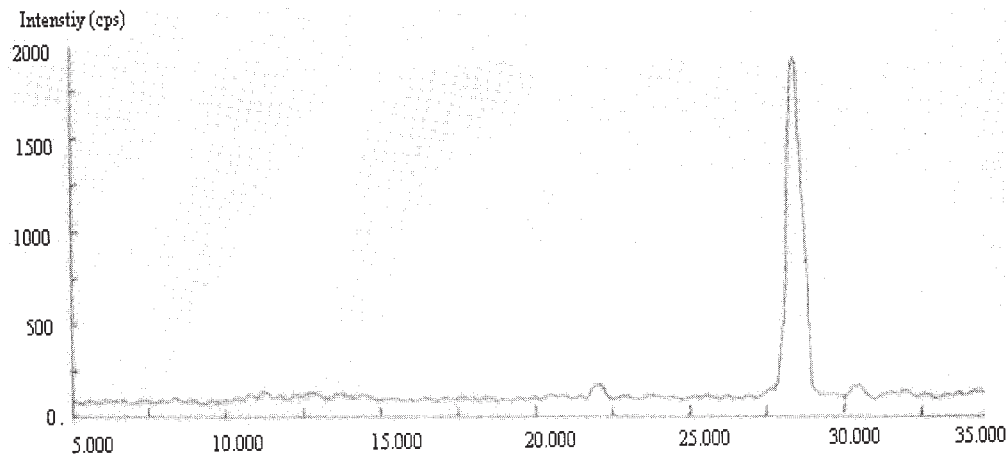
An analytical balanced equipped with a stationary support for an immersion vessel above or below the balance pan was used for specific gravity measurement per ASTM D 792. Corrosion-resistant wire for suspending the specimen and a sinker for a lighter specimen with a specific gravity of less than 1 were employed. A beaker was used as an immersion vessel, a test specimen of convenient size was weighed in air, and then the specimen was suspended from a fine wire attached to the balance. The sample was completely immersed in distilled water. The weight of the specimen in water was determined (with the sinker). The specific gravity of the specimen was calculated as follows:

$$\text{Specific gravity of specimen} = \frac{a}{(a + w) - b} \quad (1)$$

where *a* is the weight of the specimen in air, *b* is the weight of the specimen (with the sinker) and wire in water, and *w* is the weight of the totally immersed sinker and partially immersed wire.

**Flame retardancy**

A flame-retardancy test was carried out on a flame tester (prolific make) per ASTM D 4804. The sample was clamped with 85 mm above the horizontal screen so that it would not sag and touch the screen. A free end was exposed to a specified gas flame for 30 s. The



(c)

Figure 2 (Continued from the previous page)

sample was clamped at a 45° angle with the flame tip. The time required for burning and the relative rate of burning were measured.

### Swelling index

The swelling index, an indirect way of measuring the total crosslink density, which in turn can be correlated with the physical properties of the various vulcanizates, was determined by the swelling of a piece of the sample in toluene for 24 h at room temperature. It was calculated with the following equation:

$$\text{Swelling index} = \frac{X - Y}{Y}$$

where  $X$  is the weight of the sample after swelling and  $Y$  is the weight of the sample before swelling.

### Abrasion resistance index

An abrasion resistance index test was carried out on a rotating drum abrasion tester (prolific make) per the IS 3400 standard. A test specimen of  $16 \pm 0.2$  mm was gripped in a specimen holder in such a manner that it projected  $2 \pm 0.2$  mm beyond the face on the grip. The cylinder was rotated at 40 rpm.

## RESULTS AND DISCUSSION

### XRD characterization of nano-CaCO<sub>3</sub> particles

The yields of nano-CaCO<sub>3</sub> particles were recorded to be 87, 65, and 55% for molar ratios of 4 : 1, 20 : 1, and 32 : 1 PEG/CaCl<sub>2</sub>, respectively. Figure 2(a–c) shows XRD grams of CaCO<sub>3</sub> synthesized in PEG. The particle size distributions of nano-CaCO<sub>3</sub> were also measured

with Scherrer's formula<sup>14,17,18</sup> and were recorded to be 21, 15, and 9 nm for the 4 : 1, 20 : 1, and 32 : 1 PEG/CaCl<sub>2</sub> ratios, respectively. Scherrer's formula is as follows:

$$d(\text{Å}) = k\lambda / \Delta 2\theta \cos \theta \quad (3)$$

where  $d$  is the particle size,  $k$  is the order of reflection,  $\lambda$  is 1.542,  $\theta$  is the diffraction angle, and  $\Delta 2\theta$  is the full width at half-maximum. With an increasing molar ratio of PEG, the nanosize decreased. The XRD peaks became broader, and this was a major indication of a reduction in the nanosize. The peak broadening may have been due to vigorous mixing at the molecular level.

### Swelling index

The swelling indices of different filler composites are shown in Figure 3. The swelling index of nano-CaCO<sub>3</sub> with an extender decreased in comparison with that of nano-CaCO<sub>3</sub> without an extender. Also, 9-nm CaCO<sub>3</sub> showed a greater reduction in the swelling index than the other two sizes (21 and 15 nm) with linseed oil as an extender. With 10 wt % filler, the swelling indices were 2.11 and 2.32 for 9-nm and commercial CaCO<sub>3</sub>, respectively. At the same weight percentage of the filler, the swelling indices were 2.11 and 2.24 for 9-nm CaCO<sub>3</sub> with and without an extender. This was due to the greater crosslinking of rubber, as the uniform dispersion of nano-CaCO<sub>3</sub> brought the chains closer and kept them intact with nanoparticles.

### Specific gravity

The specific gravity of different filler compositions is shown in Figure 4. There was a continuous increase in

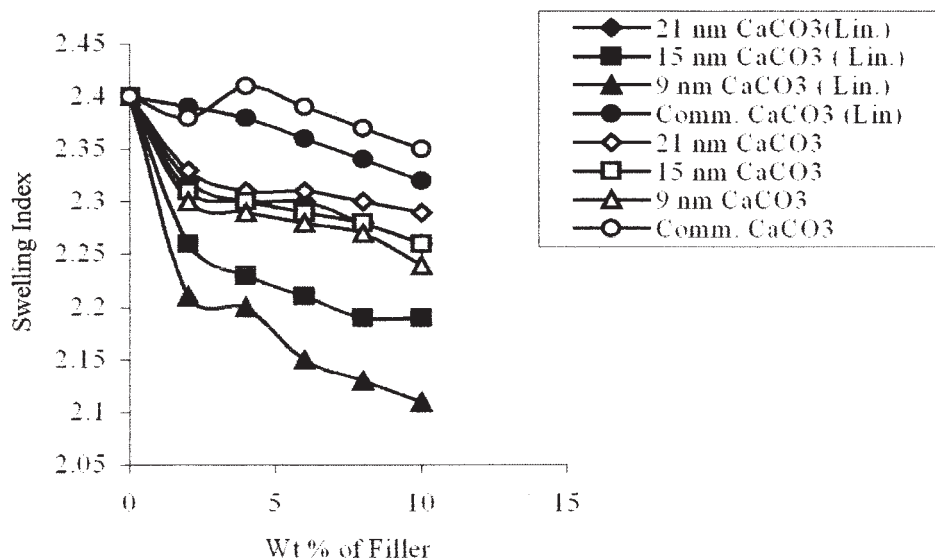


Figure 3 Swelling index of SBR filled with different fillers at various compositions.

the specific gravity for all compositions in comparison with pure SBR. The increase in the specific gravity was more appreciable for 9-nm CaCO<sub>3</sub> with linseed oil as an extender than for nano-CaCO<sub>3</sub> without an extender. The reduction in the nanosize also increased the specific gravity for the same amount of filler. With 10 wt % filler, the specific gravity was 1.68 and 1.34 for 9-nm CaCO<sub>3</sub> and commercial CaCO<sub>3</sub>, respectively, with linseed oil as an extender. This increase in the specific gravity was more pronounced than that of pure SBR (0.93). The increase in the specific gravity with a reduction in the nanosize was due to the greater and uniform dispersion of the filler in the matrix, which kept the rubber chains intact upon crosslinking.

**Tensile strength**

The relationship between the weight percentage of the filler and the tensile strength of SBR/filler composites is shown in Figure 5. The tensile strength of the nano-CaCO<sub>3</sub> rubber composites with linseed oil as an extender was higher than that of the composites without an extender up to 8 wt % filler. All the filler compositions showed the maximum value of the tensile strength at an 8 wt % filler loading and beyond that a reduction. At an 8 wt % loading of the 9-nm CaCO<sub>3</sub> filler, the tensile strength was recorded to be 3.89 and 2.11 MPa with and without an extender, respectively. The increase in the tensile strength was more in 9-nm CaCO<sub>3</sub> than in the other two sizes, that is, 21 and 15

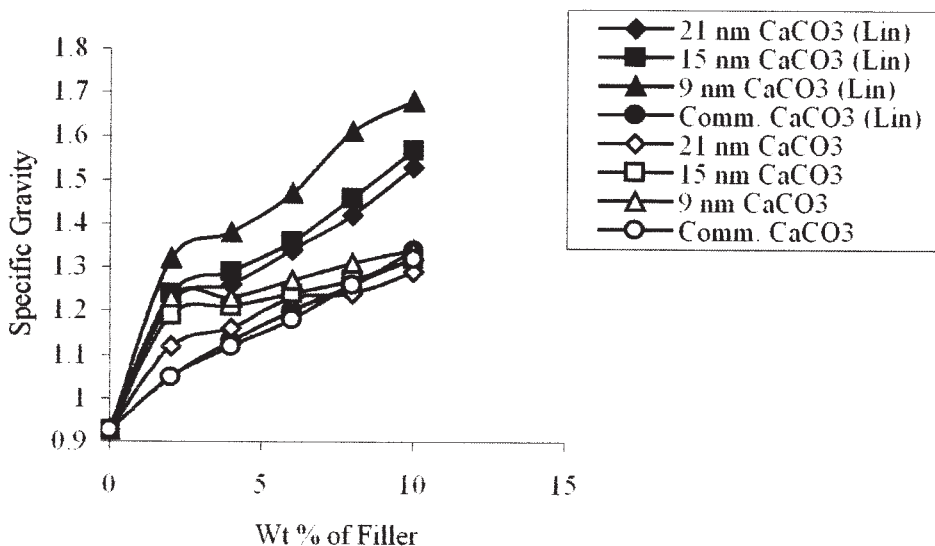
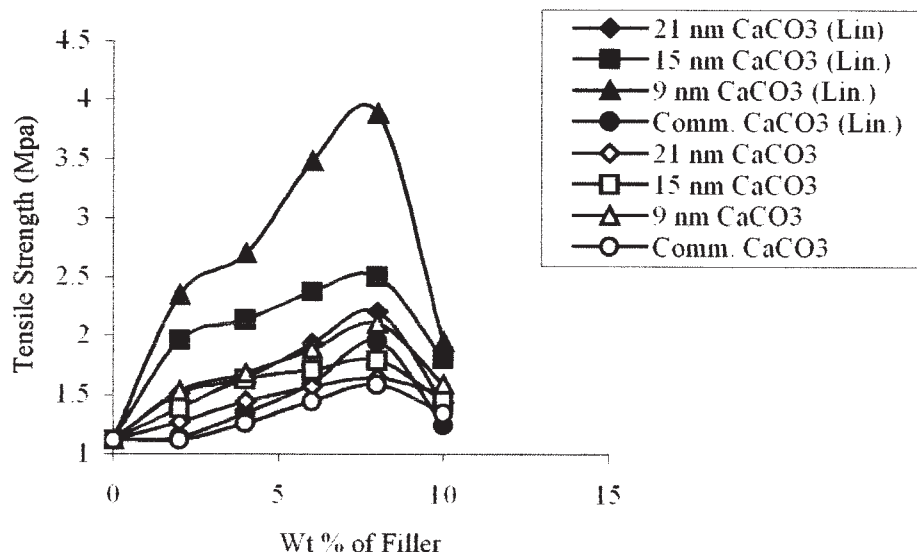


Figure 4 Specific gravity of SBR filled with different fillers at various compositions.





**Figure 5** Tensile strength of SBR filled with different sizes of CaCO<sub>3</sub> fillers at various compositions.

nm, with an extender. In comparison with pure SBR (1.12 MPa), 9-nm CaCO<sub>3</sub> with an extender showed the highest increase in the tensile strength. This was due to the linseed oil used as an extender, which helped with the uniform dispersion of nano-CaCO<sub>3</sub> in the rubber matrix, which resulted in an intercalation phenomenon.<sup>19</sup> Above an 8% composition, the results for the nanofiller were not appreciable because the nanoparticles agglomerated at a higher percentage of calcium carbonate (i.e., filler–filler interaction). This phenomenon was also observed in optical photographs [Fig. 6(a,b)].

#### Modulus at 300%

The modulus at 300% elongation increased for all composites up to an 8 wt % filler loading (Fig. 7). This property was more appreciable for nano-CaCO<sub>3</sub> with an extender than for nano-CaCO<sub>3</sub> without an extender. Also, the modulus at 300% elongation showed the highest increase for 9-nm CaCO<sub>3</sub> in comparison with the other two sizes (21 and 15 nm) with an extender.

Up to an 8 wt % filler loading, the modulus at 300% elongation increased with an increasing amount of the filler, with and without an extender. The results for the modulus at 300% elongation with an extender were significantly higher than those for the modulus without an extender for all compositions. This was due to the uniform dispersion, which was more pronounced with an extender than without one, as the extender reduced the viscosity of masticated rubber and, upon vulcanization, the rubber chains came into contact with nanoparticles. Thus, the modulus increased. Above an 8 wt % filler loading, the modulus decreased. This was due to the agglomeration of filler particles.

#### Elongation at break

Figure 8 illustrates the elongation at break of nano-CaCO<sub>3</sub> and commercial CaCO<sub>3</sub> with and without lin-

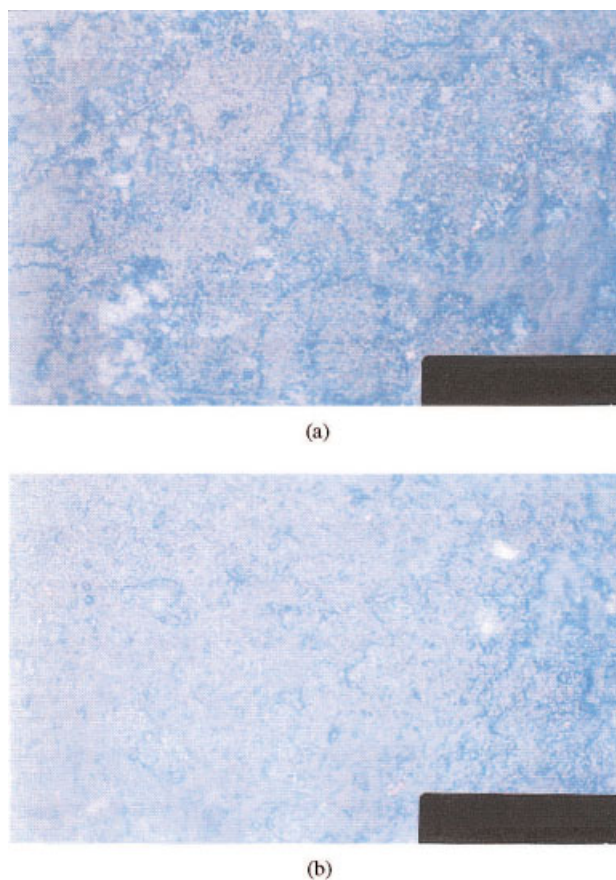


**Figure 6** Optical photographs of SBR filled with nano-CaCO<sub>3</sub> at (a) 10 and (b) 8 wt %. [Color figure can be viewed in the online issue, which is available at [www.interscience.wiley.com](http://www.interscience.wiley.com).]

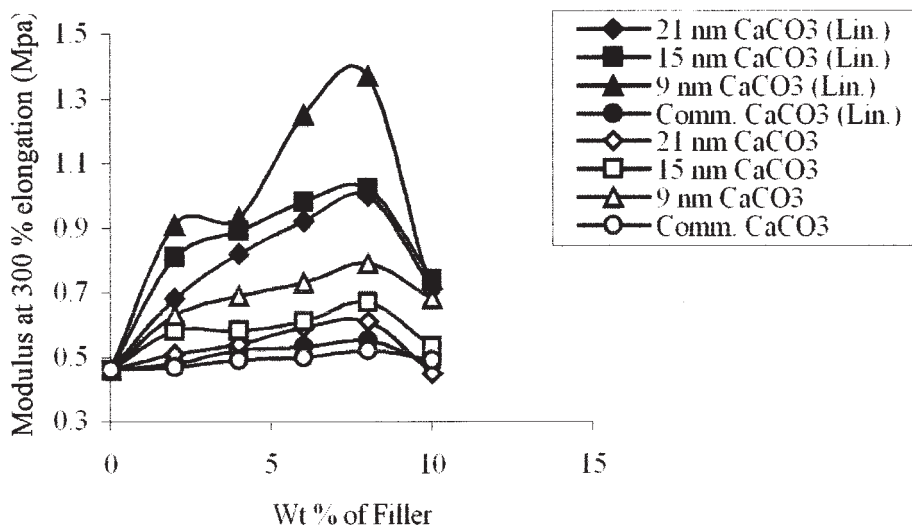


Figure 7 Modulus at 300% elongation of SBR filled with different fillers at various compositions.

seed oil. For all compositions, the elongation at break increased with an increase in the filler content up to 8 wt %. For all nanosizes of CaCO<sub>3</sub> (21, 15, and 9 nm), the increase in the elongation was significantly greater than that of the commercial CaCO<sub>3</sub> (with an extender). However, the elongation at break increased with a decrease in the nanosize for all cases. With 8 wt % 9-nm CaCO<sub>3</sub> filler, the values of the elongation with and without an extender were recorded as 824.07 and 565%. In comparison with pure SBR, the increases in the values of 8 wt % commercial and 9-nm CaCO<sub>3</sub> were 138 and 338%, respectively (i.e., significantly higher for 9-nm CaCO<sub>3</sub>).

There was a continuous increase in the hardness with an increase amount of the filler for all compositions. The increase in the hardness was more pronounced for nano-CaCO<sub>3</sub>-filled SBR than for commercial CaCO<sub>3</sub>. Also, the hardness increase was higher (i.e., 73) for 9-nm-CaCO<sub>3</sub>-filled SBR than for the other two sizes of CaCO<sub>3</sub> (63 for 21-nm CaCO<sub>3</sub> and 67 for 15-nm CaCO<sub>3</sub>). In comparison with pure SBR, the increase in the hardness in 9-nm CaCO<sub>3</sub> was recorded to be 137% higher with 10 wt % filler, whereas for the same weight percentage of commercial CaCO<sub>3</sub>, it was 111% higher. The hardness increase was greater in all cases with an extender in comparison with those without an extender.

**Hardness**

Figure 9 shows the hardness of CaCO<sub>3</sub>-filled SBR with different compositions and various sizes of CaCO<sub>3</sub>.

**Abrasion resistance index**

Figure 10 shows the abrasion resistance index of nano-CaCO<sub>3</sub> and commercial CaCO<sub>3</sub> filled in SBR with and

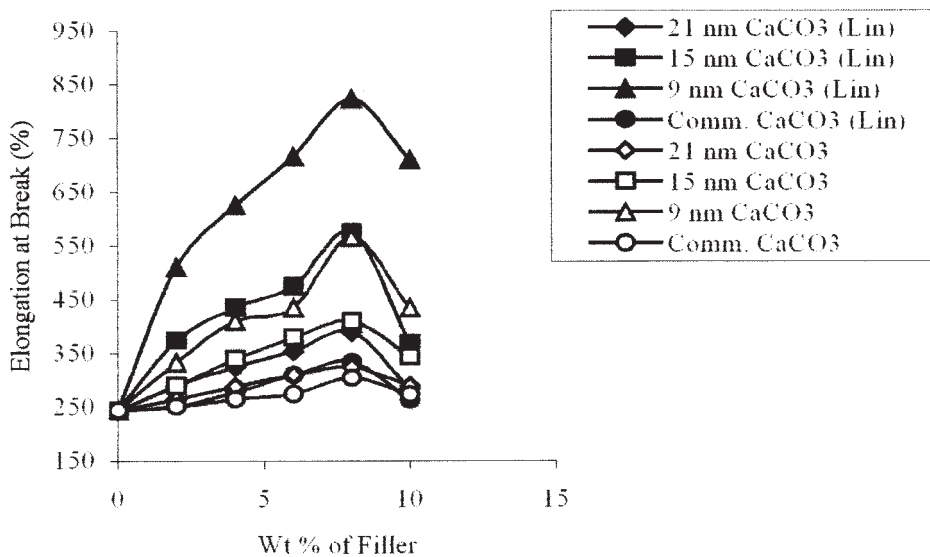


Figure 8 Elongation at break of SBR filled with different sizes of CaCO<sub>3</sub> fillers at various compositions.

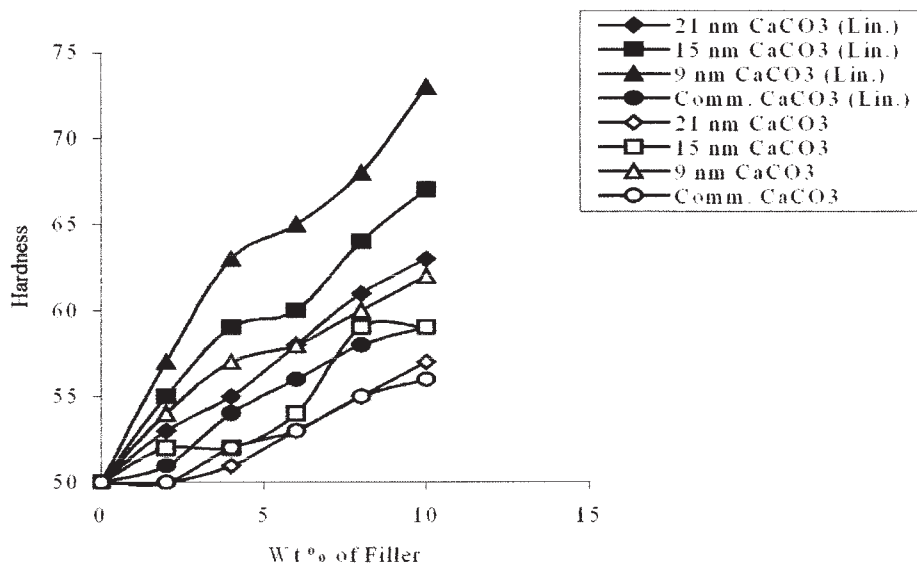


Figure 9 Hardness of SBR filled with different fillers at various compositions.

without linseed oil as an extender. The abrasion resistance increased with an increase in the filler concentration from 0 to 10 wt % for all cases in comparison with pure SBR. However, the maximum increase in the abrasion resistance was observed in 9-nm-CaCO<sub>3</sub>-filled SBR with linseed oil at 10 wt %; 9-nm CaCO<sub>3</sub> showed abrasion resistance indices of 0.27 and 0.34 with and without an extender, respectively. Also, 9-nm CaCO<sub>3</sub> showed a reduction in the abrasion resistance index in comparison with the other two sizes. For 21- and 15-nm CaCO<sub>3</sub> with an extender, the abrasion resistance indices were 0.34 and 0.28, respectively.

### Flammability

The rate of burning of different filler compositions is shown in Figure 11. Nanosize-CaCO<sub>3</sub>-filled rubber

with an extender showed a significant reduction in flammability in comparison with that without an extender. The nanofiller formed an effective layer on the surface by its uniform dispersion with linseed oil as an extender. The rate of flame retarding of nano-CaCO<sub>3</sub> was more than that of commercial CaCO<sub>3</sub> with linseed oil. In this case, the rate of flame retarding for 9-nm CaCO<sub>3</sub> was 2.55 s/mm, whereas for commercial CaCO<sub>3</sub> it was 1.78 s/mm. The increase in flame retardancy with a decrease in the size was due to the uniform dispersion of the nanosize, which resulted in greater absorption of heat energy.

In light of the results for the specific gravity, swelling index, tensile strength, modulus at 300% elongation, elongation at break, hardness, abrasion resistance index, and flame-retardancy properties, the improvement in the properties was phenomenal with a reduc-

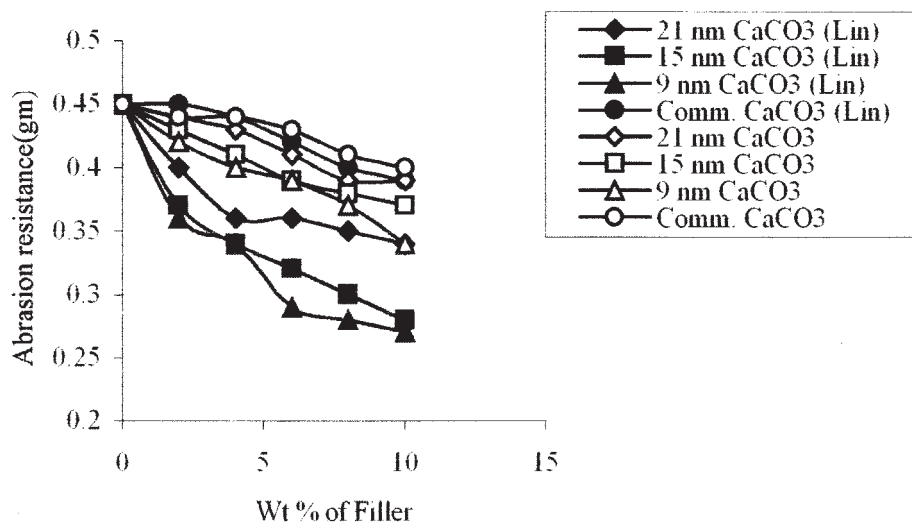


Figure 10 Abrasion resistance of SBR filled with different fillers at various compositions.



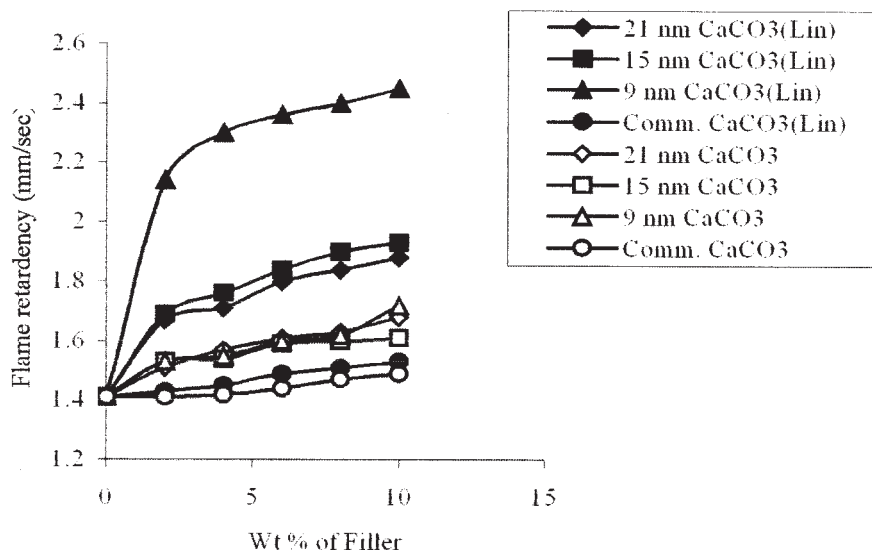


Figure 11 Rate of burning of SBR filled with different fillers at various compositions.

tion in the nanosize and the use of an extender. Therefore, it can be asserted that the use of linseed oil enhanced the uniform dispersion of nanoparticles, which covered the whole matrix in a broader way by their smaller size and higher surface area. Thus, the large extent of rubber intercalation into the nanoparticles provided a strong rubber–filler interaction. Up to 8 wt % filler, the dispersion of nanoparticles was greater. Further chances of agglomeration were there.<sup>20</sup> The optical micrographs [Fig. 6(a,b)] showed that a higher amount of the filler produced bigger particles in comparison with less filler.

## CONCLUSIONS

Nano-CaCO<sub>3</sub> particles were synthesized in three different nanosizes with an *in situ* deposition technique. Among the four systems studied, the 9-nm-CaCO<sub>3</sub>-filled SBR showed better enhancement of the properties in comparison with commercial and other nanosizes of CaCO<sub>3</sub>. This was due to a reduction in the nanosize. The linseed oil used as an extender helped with the homogeneous mixing of nanoparticles in the rubber matrix, which intercalated the rubber to a large extent into the nanoparticles and provided a strong rubber–filler interaction. The strong rubber–filler interaction increased the physical, mechanical, and thermal properties of the composites.

## References

- Zhang, L.; Wang, Y.; Wang, Y.; Sui, Y.; Yu, D. *J Appl Polym Sci* 2000, 78, 1873.
- Lopez-Manchado, M. A.; Herrero, B.; Arroyo, M. *Polym Int* 2003, 52, 1070.
- Philipp, G.; Schmidt, H. *J Non-Cryst Solids* 1984, 63, 283.
- Morikawa, A.; Iyoka, Y.; Kakimoto, M.; Imai, Y. *Polym J* 1992, 24, 107.
- Norak, B. M.; Ellsworth, M. W.; Verrier, C. *Polym Mater Sci Eng* 1993, 70, 266.
- Galaser, R. H.; Wilkes, G. C. *Polym Bull* 1989, 19, 51.
- Pope, E. J. A.; Asami, A.; Makenzie, J. D. *J Mater Res* 1989, 4, 1018.
- Yingwei, D. I.; Iannace, S.; Maio, E. D. I.; Nicolais, L. *J Polym Sci Part B: Polym Phys* 2003, 41, 670.
- Kim, J.-T.; Oh, T.-S.; Lee, D. H. *Polym* 2003, 52, 1058.
- Saujanya, C.; Radhakrishnan, S. *Polymer* 2001, 42, 6723.
- Dagani, R. C. *E News* 1999, 77(23), 25.
- Godovski, Y. D. *Adv Polym Sci* 1999, 119, 79.
- Sherman, L. M. *Plast Technol* 1999, 45, 53.
- Saujaya, C.; Radhakrishnan, S. *J Mater Sci* 1998, 33, 1069.
- Saujanya, C.; Ashmol Radhakrishnan, S. *Polym Commun* 2000, 42, 2257.
- Mishra, S.; Sonawane, S. H.; Singh, R. P.; Bendale, A.; Patil, K. *J Appl Polym Sci* 2004, 94, 116.
- Pathak, A.; Panda, A. B.; Tarafdar, A.; Pramanik, P. *J Indian Chem Soc* 2003, 80, 289.
- Mishra, S.; Sonawane, S. H.; Singh, R. P. *J Polym Sci Part B: Polym Phys* 2004, 43, 107.
- Chang, Y.-W.; Yang, Y.; Ryu, S.; Nah, C. *Polym Int* 2002, 51, 319.
- Xiong, M.; Wu, L.; Zhou, S.; You, B. *Polym Int* 2002, 51, 693.